

CONF-961202--8

Note: This is a preprint of a paper being submitted for publication. Contents of this paper should not be quoted nor referred to without permission of the author(s).

To be submitted to the 1996 Fall MRS meeting

Optical and Structural Characterization of Zinc Implanted Silica Under Various Thermal Treatments

R. Mu, J. Chen, Z. Y. Gu, A. Ueda, Y.-S. Tung, and D. O. Henderson
Fisk University
Nashville, TN

C. W. White, J. G. Zhu, J. D. Budai, and R. A. Zuhr
Oak Ridge National Laboratory
Oak Ridge, TN

"The submitted manuscript has been authored by a contractor of the U.S. Government under contract No. DE-AC05-96OR22464. Accordingly, the U.S. Government retains a nonexclusive, royalty-free license to publish or reproduce the published form of this contribution, or allow others to do so, for U.S. Government purposes."

RECEIVED
DEC 3 1 1996
OSTI

Prepared by the
Oak Ridge National Laboratory
Oak Ridge, Tennessee 37831
managed by
LOCKHEED MARTIN ENERGY RESEARCH CORP.
for the
U.S. DEPARTMENT OF ENERGY
under contract DE-AC05-96OR22464

MASTER

December 1996

DISTRIBUTION OF THIS DOCUMENT IS UNLIMITED

m

DISCLAIMER

This report was prepared as an account of work sponsored by an agency of the United States Government. Neither the United States Government nor any agency thereof, nor any of their employees, makes any warranty, express or implied, or assumes any legal liability or responsibility for the accuracy, completeness, or usefulness of any information, apparatus, product, or process disclosed, or represents that its use would not infringe privately owned rights. Reference herein to any specific commercial product, process, or service by trade name, trademark, manufacturer, or otherwise does not necessarily constitute or imply its endorsement, recommendation, or favoring by the United States Government or any agency thereof. The views and opinions of authors expressed herein do not necessarily state or reflect those of the United States Government or any agency thereof.

DISCLAIMER

**Portions of this document may be illegible
in electronic image products. Images are
produced from the best available original
document.**

OPTICAL AND STRUCTURAL CHARACTERIZATION OF ZINC IMPLANTED SILICA UNDER VARIOUS THERMAL TREATMENTS

R. MU*, JINLI CHEN*, Z.Y. GU*, A. UEDA*, Y.-S. TUNG*, D.O. HENDERSON*, C.W. WHITE**, JANE G. ZHU**, JOHN D. BUDAI AND R.A. ZUHR**

*Chemical Physics Laboratory, Department of Physics, Fisk University, Nashville, TN

**Solid State Division, Oak Ridge National Laboratory, Oak Ridge, TN

ABSTRACT

Zinc ion implanted silica with controlled thermal annealing has been investigated. Low temperature optical measurements indicate the presence of Zn clusters in the as-implanted silica. Optical spectra of the annealed sample under a reducing environment suggest Zn cluster and Zn metal colloid formation. The absorption peak at ~5.3 eV may be due to the surface plasma absorption of Zn metal colloids in silica. The oxidized samples (10 and 6×10^{16} ions/cm 2) show an absorption peak at ~4.3 and ~4.8 eV, respectively and imply ZnO quantum dot formation. The blueshift in exciton absorption can be attributed to the quantum confinement effects.

INTRODUCTION

It is conceivable that the study of physical and optical properties of nanophase materials assembled in various solid hosts can eventually lead to revolutionary changes in electronic, optical and telecommunication industries. However, the present understanding of nanophase materials, such as metal colloids and quantum dots, is far from comprehensive due to the complex structural, physical and optical modifications of the nanophase materials themselves from their bulk and multiplex interactions between the confining host and the confined materials. Depending upon the physical properties of the confining hosts and the nature of the confined materials, many unique mechanical, thermal and optical properties have been observed and are related to different types of confinement effects.¹⁻⁷ For example, 1) the physical confinement, the interfacial interaction between guest and host and the reduction of the physical size of the confined particles can lead to *a*) hardness modification of materials;¹ *b*) depression of the melting and freezing transition temperatures;² and *c*) alteration of crystal nucleation and growth characteristics;³ 2) the quantum confinement of free electrons in metals and excitons in semiconductors can result in the observation of the surface plasma resonance (SPR) and the shifts of the band gap;^{4,5} 3) dielectric confinement gives rise to surface phonons observed in a wide range of nanophase materials.^{6,7} Due to the fact that quantum and dielectric confinement effects typically occur simultaneously it is difficult to identify the relative contributions to each of these effects.

Optical properties of Zn and zinc oxide materials have been well documented in literature.⁸⁻¹⁰ Zinc oxide is a typical wide band gap metal oxide semiconductor material. Like indium tin oxide (ITO), a proper doping of ZnO semiconductor film can result in a electrical conducting and optical transparent film, which has very important applications in flat panel display technology. In addition, the synthesized ZnO nanoparticles display many unique optical properties both in excitonic transitions and surface phonon modes due to the quantum confinement of excitons for small particles ($R_{\text{particle radius}} < a_B$ (Bohr exciton radius))^{7,8,10} and to the dielectric confinement from the mismatch of the dielectric functions between the host and the confined nanoparticles.^{6,7}

The effort made in the present work is first to utilize ion implantation to inject low melting metal, Zn, into optical grade fused silica. Then, the Zn implanted silica substrates are thermally and laser annealed under reducing ($H_2 + Ar$) and oxidizing ($O_2 + Ar$) environments or in air to produce Zn metal colloids and ZnO semiconductor quantum dots. Optical characterizations are conducted to understand metal and metal oxide clusters and nanoparticle formation and growth kinetics. Vibrational infrared spectroscopy is used to study surface phonon modes of ZnO nanocrystals in a silica host. It is also intended that a controllable and a new interface may be created such as Zn colloids coated with a zinc oxide shell or zinc oxide quantum dots coated with a Zn metal shell by alternating the annealing conditions from reducing to oxidizing atmosphere and vice versa.

EXPERIMENTAL

Optical grade fused silica (Corning 7940) was used as the substrate. Zn ions with ion energies of 160 keV were injected into the substrate. Based upon Rutherford Back-Scattering (RBS) measurement followed by TRIM simulation, the Zn ion distribution in silica substrates form almost a perfect Gaussian shape with the peak position of $0.12 \pm 0.01 \mu m$ below the substrate surface. Four nominal doses were implanted in silica substrates. They are 1, 3, 6, and 10×10^{16} ions/cm². At the peak of the Gaussian, volume filling fraction of Zn in silica is $\sim 2-3\%$ for the highest dose.

In order to fabricate Zn colloids and to study the colloid formation kinetics and the properties of the ion damaged silica substrates, a stepwise (every 100 °C) thermal annealing process is adopted. The samples were first annealed under reducing ($H_2 + Ar$) atmosphere and then under oxidizing ($O_2 + Ar$) environment. It is expected that Zn metal colloids will be formed under former condition, while zinc oxide semiconductor quantum dots or the oxide coated Zn metal colloids will be the major products resulting from annealing in the later condition. The starting and the ending annealing temperatures were 200 and 700 °C, respectively. At 700 °C, a clear decrease in absorption intensity is observed indicating the loss of Zn. Then these samples were annealed under oxidizing environment. After each step of annealing, both optical (infrared and UV-Vis) and surface (Optical and Atomic Force) microscopic characterizations were conducted to monitor the changes.

Optical measurements were made with a Hitachi 3501 UV-Vis-NIR spectrophotometer in the range of 3200 - 185 nm (0.38 - 6.7 eV) in both transmittance and reflectance modes. 0.1 nm spectral resolution was used for low temperature measurements and 1.0 nm resolution for room temperature measurements. Infrared spectra were collected with Bomem MB102 and DA3 spectrometers with a resolution of 4 cm⁻¹.

In order to examine any possible small Zn cluster formation in the low dose Zn implanted silica, low temperature optical measurements were conducted with a Janis closed cycle CCS-300 refrigerator equipped with a Lakeshore Cryotronics 320 temperature controller. Selected samples were examined between 8 - 300 K and the temperature was controlled within 0.5 K for each run.

RESULTS

Fig. 1 shows the extinction UV-Vis spectra of the as-implanted optical grade silica with nominal Zn doses of 1, 3, 6 and 10×10^{16} ions/cm². When the ion dose is higher than 3×10^{16} ions/cm², a broad peak at ~ 5.1 eV is clearly defined. Fig. 2 displays the UV-Vis spectra of Zn as-implanted silica substrate at room temperature and 8 K with the photon energy above 5.0 eV.

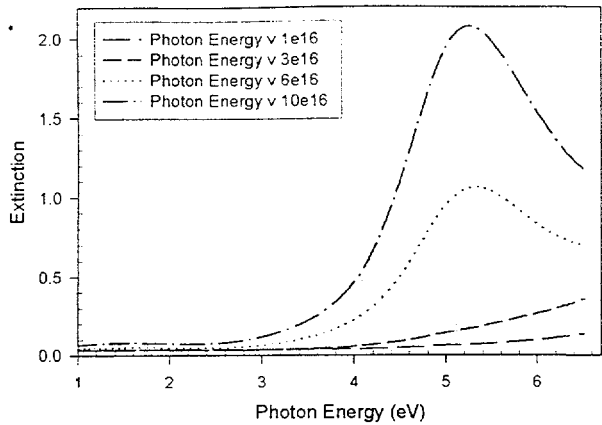


Fig. 1 Optical spectra of as-implanted silica with Zn concentration of 1, 3, 6 and 10×10^{16} ions/cm².

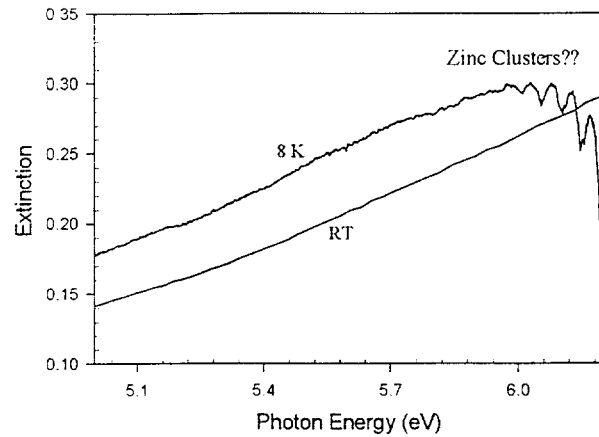


Fig. 2 Optical spectra of Zn implanted silica with dose of 3×10^{16} ions/cm² at 8 and 300 K. A set of fine structure at photon energy $E \geq 6.0$ eV is observed.

At room temperature, the extinction spectrum is featureless. However, when the system is cooled down to 8 K, a series spectral peaks is observed. The separation of these peaks are ~ 2 nm apart. In addition, these features are only observed in 3×10^{16} ions/cm² implanted samples. Fig. 3 illustrates two sets of thermally annealed Zn implanted samples with doses of 3 and 10×10^{16} ions/cm² in a reducing atmosphere and annealed at temperatures of 300 - 700 °C. A common feature is that as the temperature increases, the absorption cross-section between 5 - 6 eV is increased. In the case of 3×10^{16} ions/cm², the center peak is redshifted from ~ 6.0 eV down to 5.5 eV. However, an opposite spectral shift is observed for the dose of 10×10^{16} ions/cm², i.e., the center peak at ~ 5.2 eV is blueshifted up to 5.4 eV as the annealing temperature is increased. Fig. 4 illustrates a set of changes in a spectra when samples were annealed under a hydrogen environment at 700 °C and then annealed in an oxygen atmosphere. Clearly, the absorption intensity at ~ 5.6 eV is decreased and the absorption at ~ 4.3 eV is enhanced for the dose of 10×10^{16} sample. A similar trend is also observed for the 6×10^{16} sample. It should be noted that the center of the intensity reduction is the same energy as the 10×10^{16} sample, but the center of the enhanced intensity is at 4.7 eV; i.e., the center of the enhanced peak position is blueshifted as the ion dose decreases.

DISCUSSION

It is known that when silica is implanted

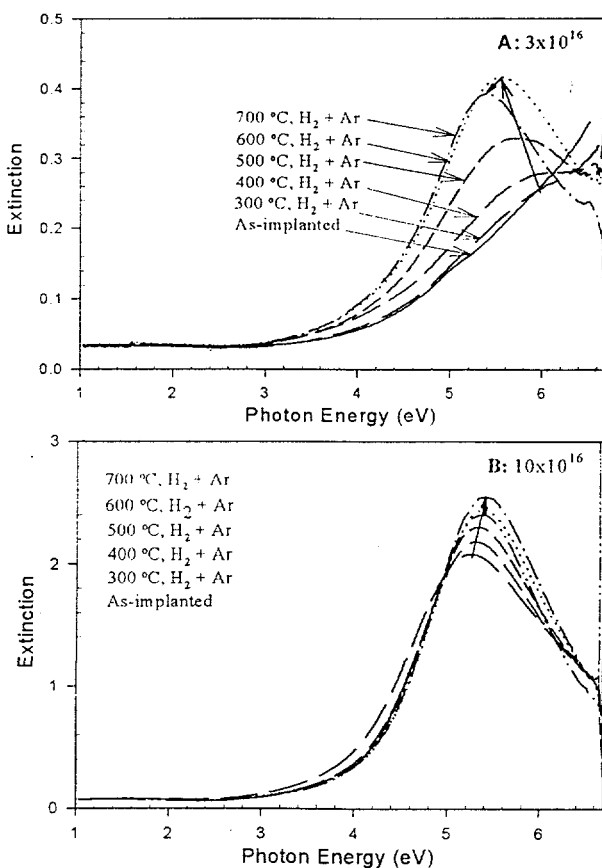


Fig. 3 Optical spectra show thermal annealing effects on Zn implanted fused silica under H₂ + Ar environment. A) 3×10^{16} ions/cm²; B) 10×10^{16} ions/cm².

with energetic ions, a few bands are expected to be observed in the deep UV region, which have been attributed to the defect centers created by the energetic ions.¹¹ The creation of defect centers in a silica host has been further illustrated by EPR and infrared techniques.¹¹⁻¹³ Therefore, it is logical to consider the ion dose dependent absorption tail near 6.2 eV is due to the creation of the defect centers in the silica host. However, as is shown in fig. 1, the quick spreading of the absorption tail into visible region indicates that an additional optical absorption center(s) is also present. It is expected that as the Zn concentration increases, Zn clusters can also be formed. Schroder *et al.*¹⁴ have investigated the optical spectra of Ne matrix-isolated Zn_n ($n \leq 6$). As the concentration of the Zn in the Ne matrix increases, more and more absorption peaks are observed. The spreading of the absorption bands is progressively into near UV region. At the concentration of 0.002%, only one strong peak is observed at ~ 6 eV, which is attributed to Zn atoms. As the concentration increases, more and more absorption bands are observed. At the concentrations of 2.8

and 10.2%, the absorption spectra look very similar to each other and they are able to fit the spectrum at 10.2% with a linear combination of Zn_1 - Zn_6 absorption spectra. Based on the RBS data from Zn implanted silica, the peak concentration of Zn at the nominal dose of 10×10^{16} ions/cm² is estimated to be $\sim 3\%$. Therefore, a similar absorption spectrum may be expected and is superimposed on to the absorption spectrum due to the defect centers in silica. For larger Zn clusters, a surface plasma absorption of Zn colloids is also expected.¹⁵ Based on Mie scattering theory, our calculation suggests a strong surface plasma absorption should occur above 3.5 eV when the Zn concentration is more than 0.1%. Based on the similarity of the Zn concentrations used in Schroder's work and our ion implanted doses, we would expect the two spectra resemble one another with exception to the ion induced defects in silica. Therefore, it is reasonable to assume that the dose dependent broad band absorption below 5 eV can be due to both defect centers in silica resulting from ion damage and to cluster formations of Zn in silica matrix.

Low temperature optical absorption measurements were also conducted. All other Zn doses failed to show any clear changes in the temperature range of 8 - 300 K except for the one with dose of 3×10^{16} ions/cm². It is evident that fine structure can be observed when the sample is cooled down to 8 K as shown in fig. 2. This structure is highly reproducible and disappears when the sample is warmed up to room temperature. Many experiments on various samples with the same and different Zn concentrations enable us to rule out any conceivable experimental artifacts. We can also discount the possibility that fine structure results from interference fringes. This is based on the fact that an equivalent film thickness of 6 μm is required to produce the oscillations observed in UV for the 3×10^{16} sample (an index of 1.5 was used for the calculation). We,

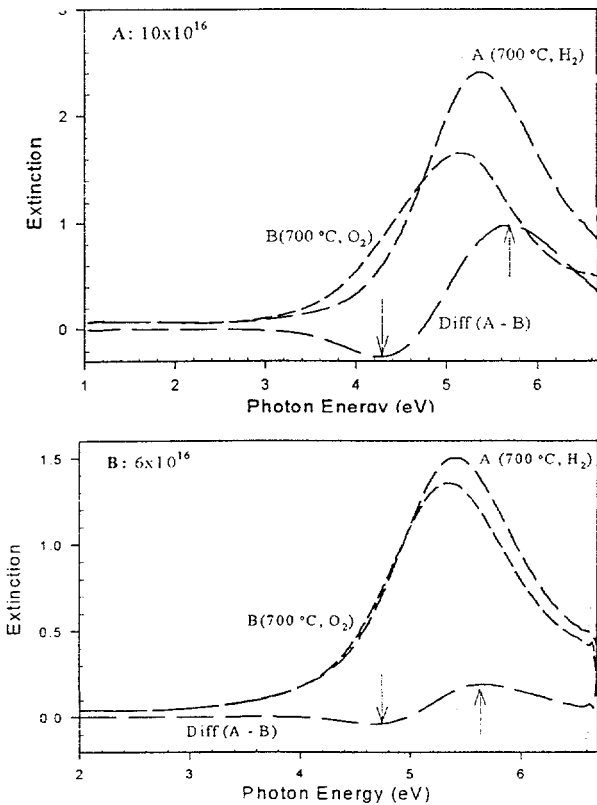


Fig. 4 Difference spectra of Zn implanted silica thermally annealed under H_2 (700 °C, 30 min.) and then annealed under O_2 (700 °C, 30 min.) A) 10×10^{16} ions/cm², and B) 6×10^{16} ions/cm².

therefore, conclude that the sharp peaks observed at low temperature are due to the sample itself and tentatively attributed them to absorption of Zn clusters. However, more experiments are required to confirm this speculation. It is also conceivable that the sharp peaks could be due to vibrational fine structure that is resolved in the electronic transition at low temperature. In the latter case, we have to assume that the electronic transition peak is above 6.6 eV so that the stronger absorption phonon bands peaks are the low order.

Thermal annealing at temperatures of 300 - 700 °C under 5%H₂ + 95%Ar further supports the idea of Zn cluster formation in the as-implanted samples shown in fig. 1. It is known that thermal annealing at high temperature can eliminate defect centers created by ion implantation in silica. If the absorption below 4.5 eV was Solely due to these defects resulting from ion damage, then one would have observed a progressive decrease in absorption since more and more defects are thermally removed.^{11,12} This is also supported by our infrared reflectance spectra of the ion implanted silica. However, our observation is to the contrary. As the temperature and thermal annealing time are increased, the absorption intensity is enhanced and the peak position is redshifted. As pointed out earlier, Zn metal colloids and small clusters can absorb photons in 4 - 6 eV. Therefore, it is believed that the increase in intensity upon annealing is primarily due to the formation of Zn clusters and metal colloids. By comparing the dose and temperature dependent thermal annealing results in fig. 3, the redshift (3×10^{16} ions/cm²) and the blueshift (10×10^{16} ions/cm²) of the absorption peak suggest Zn colloid formation in silica. In addition, the surface plasma of the Zn metal colloids is located at ~5.3 eV. The redshift for lower dose of 3×10^{16} ions/cm² is mainly due to the transition from Zn cluster to metal colloids, while the blueshift for higher dose of 10×10^{16} ions/cm² is predominantly due to the reduction of the defect centers in the host materials.

When the samples are annealed under a reducing atmosphere and further treated under oxidizing environment at 700 °C, a clear spectral band shift is observed. The these spectra, as illustrated in fig. 4, clearly show that an additional peak at ~4.3 and ~4.7 eV has developed with the expense of the intensity at ~5.6 eV for the Zn doses of 10 and 3×10^{16} ions/cm², respectively. It can be argued that when the samples are annealed under an oxygen environment, some of the Zn clusters and colloids may be oxidized and eventually form ZnO quantum dots. The physical size of these ZnO quantum dots can be closely related to the size of the Zn metal colloids. It is also know that the band gap of ZnO semiconductor is ~3.4 eV and its Bohr exciton radius $a_B = 2.5$ nm.¹⁶ It is also known that when the physical size of quantum dots is comparable or smaller than the exciton radius a_B , their exciton absorption is blueshifted, which can be qualitatively predicted by EMA theory.¹⁷ With these considerations, it is logical to consider that the physical size of the ZnO quantum dots formed in higher dose (10×10^{16} ions/cm²) is larger than that of the lower dose (3×10^{16} ions/cm²) and consequently the absorptions at ~4.3 and ~4.7 eV for the oxidized samples (3×10^{16} and 10×10^{16} ions/cm²) are due to the exciton absorption of the ZnO quantum dots in the silica host.

CONCLUSION

Optical characterization of Zn ion implantation in optical grade silica with four nominal doses of 1, 3, 6 and 10×10^{16} ions/cm² with and without thermal treatments has been conducted. The strong optical absorption below 4.5 eV for the as-implanted samples is attributed both to defect centers in silica due to the ion implantation and to Zn clusters formed in silica. A set of absorption peaks at 8 K at photon energy $E \geq 6.0$ eV may be due to Zn cluster formation and/or vibrational fine structure of these clusters. Thermal annealing under 5%H₂+95%Ar shows the intensity enhancement at ~ 5.3 eV, which can be attributed to Zn cluster and metal colloid

absorption. Oxygen annealed samples show a new band developed at ~4.3 and ~4.8 eV and a decrease of intensity at ~5.6 eV for the doses of 6 and 10×10^{16} ions/cm² suggesting possible ZnO quantum dot formation. The blueshift of the exciton absorption for the lower dose from 4.3 to 4.8 eV is due to the stronger quantum confinement effects as predicted by EMA theory.

ACKNOWLEDGMENTS

Authors wish to acknowledge the supports from DOE under grant DE-FG05-94ER45521 at Fisk and contract DE-AC05-84OR21400 with Lockheed Martin Energy System at Division of Materials Science, ORNL.

REFERENCES

1. for example: R. W. Siegel, IV International Conference on Advanced Materials, IUMRS-ICAM 95, Cancun Mexico, Aug. 27 - Sept. 1995.
2. M.B. Ritter, D.D. Awschlam, W.M. Shafer, Phys. Rev. Lett. **61**, 966 (1988); J. Warnock, D.D. Awschalom, M.W. Shafer, Phys. Rev. Lett. **57**, 1753 (1986); R. Mu, F. Jin, S.H. Morgan, D.O. Henderson and E. Silberman, J. Chem. Phys. **100**, 7749 (1994); R. Mu and V.M. Malhotra, **44**, 4296 (1991).
3. R. Mu, Y. Xue and D.O. Henderson, Phys. Rev. B **53**, 6041 (1996); R. Mu, Y.S. Tung, A. Ueda and D.O. Henderson, J. Phys. Chem. [in print] (1997).
4. P. Mulvaney, Langmuir **12**, 788 (1996).
5. J.A.A.J. Perenboom, P. Wyder and F. Meier, Phys. Rep. **78**, 173 (1981).
6. S. Hayashi, Jpn. J. Appl. Phys. **23**, 665 (1984), and references therein.
7. C.W. White, J.D. Budai, J.G. Zhu, S.P. Withrow, D.M. Hembree, Jr., D.O. Henderson, A. Ueda, Y.S. Tung, R. Mu, R.H. Magruder, J. Appl. Phys. **79**, 1876 (1996); R. Mu, D.O. Henderson, Y.S. Tung, A. Ueda, C. Hall, W.E. Collins, C.W. White, R.A. Zuhr and Jane G. Zhu, J. Vac. Sci. Technol. A **14**, 1482 (1996).
8. D.W. Bahnemann, C. Kormann and M.R. Hoffmann, J. Phys. Chem. **91**, 3789 (1987).
9. M. Haase, H. Weller and A. Henglein, J. Phys. Chem. **92**, 482 (1988), and references therein.
10. S. Mahamuni, B.S. Bendre, V.J. Leppert, C.A. Smith, D. Cooke, S.H. Risbud and H.W.H. Lee, NanoStru. Mat. **7**, 659 (1996).
11. R. A. Weeks, in *Glasses and Amorphous Materials*, edited by J. Zarzicki, Chap. 6 pp311- 373 (Wiley, New York, 1992); S. Y. Park, R. A. Weeks, and R. A. Zuhr, J. Appl. Phys. **77**, 6100 (1995).
12. D. O. Henderson, M. A. George, Y. S. Tung, R. Mu, A. Burger, S. H. Morgan, W. E. Collins, C. W. White, R. A. Zuhr, and R. H. Magruder III, J. Vac. Sci. Technol. A **13**, 1254 (1995); D. O. Henderson, S. H. Morgan, R. Mu, W. E. Collins, R. H. Magruder, C. W. White, and R. A. Zuhr, Mat. Res. Soc. Symp. Proc. **316**, 451 (1994).
13. H. Hosono, J. Appl. Phys. **69**, 8079 (1990); R. A. B. Devine, J. Non-cryst. Solids **152**, 50 (1992).
14. W. Schroder, H. Wiggenhauser, W. Schrittenlacher and D.M. Kolb, J. Chem. Phys. **86**, 1147 (1987).
15. J. A. Creighton and D. G. Eadon, J. Chem. Soc. Faraday Trans. **87**, 3881 (1991).
16. G. Redmond, A. O'Keeffe, C. Burgess, C. MacHale and D. Fitzmaurice, J. Phys. Chem. **97**, 11081 (1993).
17. A. I. Ekimov, A. L. Efros, A. A. Onushchenko, Solid State Commun. **56**, 921 (1985); L. E. Brus, J. Chem. Phys. **80**, 4403 (1984).